Original Article
J Vet Sci 2017, 18(4), 487-497 · https://doi.org/10.4142/jvs.2017.18.4.487

KCHO-1, a novel herbal anti-inflammatory compound, attenuates oxidative stress in an animal model of amyotrophic lateral sclerosis

Myung Geun Kook[1,2], Soon Won Choi[1,2], Yoojin Seo[1,2], Dong Woung Kim[3], Bong Keun Song[4], Ilhong Son[5], Sungchul Kim[6,*], Kyung-Sun Kang[1,2,*]

[1]*Adult Stem Cell Research Center, College of Veterinary Medicine, and* [2]*Research Institute for Veterinary Science, College of Veterinary Medicine, Seoul National University, Seoul 08826, Korea*
[3]*Center of Integrative Medicine, Department of Internal Medicine, Wonkwang University Gwangju Hospital, and* [6]*ALS/MND Center of Wonkwang University Korean Medical Hospital, Wonkwang University Gwangju Medical Center, Gwangju 61729, Korea*
[4]*Department of Internal Medicine, School of Oriental Medicine, Wonkwang University, Iksan 54538, Korea*
[5]*Department of Neurology, Inam Neuroscience Research Center, Wonkwang Univ. Sanbon Hospital, Gunpo 15865, Korea*

Amyotrophic lateral sclerosis (ALS) is a neurodegenerative disease characterized by selective death of motor neurons in the central nervous system. The main cause of the disease remains elusive, but several mutations have been associated with the disease process. In particular, mutant superoxide dismutase 1 (SOD1) protein causes oxidative stress by activating glia cells and contributes to motor neuron degeneration. KCHO-1, a novel herbal combination compound, contains 30% ethanol and the extracts of nine herbs that have been commonly used in traditional medicine to prevent fatigue or inflammation. In this study, we investigated whether KCHO-1 administration could reduce oxidative stress in an ALS model. KCHO-1 administered to ALS model mice improved motor function and delayed disease onset. Furthermore, KCHO-1 administration reduced oxidative stress through $gp91^{phox}$ and the MAPK pathway in both classically activated microglia and the spinal cord of $hSOD1^{G93A}$ transgenic mice. The results suggest that KCHO-1 can function as an effective therapeutic agent for ALS by reducing oxidative stress.

Keywords: amyotrophic lateral sclerosis, $gp91^{phox}$, neurodegenerative diseases, oxidative stress, traditional medicine

Introduction

Amyotrophic lateral sclerosis (ALS) is a neurodegenerative disease associated with the selective motor neuron death in the spinal cord, brain stem, and motor cortex. Typical ALS patients suffer from a gradual loss of motor function caused by muscle atrophy and degeneration. To date, the main cause of ALS has not been identified, but various pathological hallmarks such as misfolded protein aggregation, mitochondrial dysfunction, glutamate excitotoxicity, and neuro-inflammation seem to be related to the development of ALS symptoms [8,28,31]. Most cases of ALS are classified as sporadic ALS (sALS), while 10% of ALS cases are inherited familial ALS (fALS). To date, studies of fALS have identified many causes of the disease such as mutations of superoxide dismutase 1 (SOD1) [32], TAR DNA binding protein (TDP-43) [29], and translocated in liposarcoma/fused in sarcoma (FUS/TLS) [21]. The SOD1, a principal intracellular antioxidant enzyme, converts superoxide radicals to hydrogen peroxide, and SOD1 mutation can lead to multiple pathogenic mechanisms in ALS especially oxidative stress [5]. In previous study, many analyses of oxidative stress in ALS have been carried out to elucidate the relationship between degenerated motor neurons and elevated oxidative stress in ALS, and the results provide evidence supporting indications that oxidative stress affects motor neuron death and other cells [5,6]. In particular, microglia have a key role during the development of neurodegeneration by catalyzing the conversion of superoxide anion to hydrogen peroxide and

Received 14 Jul. 2016, Revised 27 Dec. 2016, Accepted 7 Feb. 2017
*Corresponding authors: Tel: +82-2-880-1298; Fax: +82-2-876-7610; E-mails: kangpub@snu.ac.kr (KS Kang), kscndl@hanmail.net (S Kim)
pISSN 1229-845X
eISSN 1976-555X
Supplementary data is available at http://www.vetsci.org only.

inducing oxidative stress in the central nervous system (CNS) of ALS [4]. In particular, under certain pathological conditions microglia produce a high level of reactive oxygen species (ROS) through $gp91^{phox}$, which is one of the main sources of ROS in microglia [13,24,40]. The increase in ROS by $gp91^{phox}$ amplifies signals to produce neurotoxic factors through the MAPK pathway. Consistently, deletion of $gp91^{phox}$, which is overexpressed in ALS microglia, can improve survival of $hSOD1^{G93A}$ Tg mice [17,26,36].

Until now, various therapeutic approaches including stem cell-based clinical trials and adjustment of drug treatments have been attempted, but no significant effective and feasible therapies have been developed [8,30,38]. The novel chemical compound KCHO-1 is a natural ethanol extract obtained from traditionally used herbal combinations which include *Curcuma* (*C.*) *longa*, *Salvia* (*S.*) *miltiorrhiza*, *Gastrodia* (*G.*) *elata*, *Chaenomeles sinensis*, *Polygala* (*P.*) *tenuifolia*, *Paeonia japonica*, *Glycyrrhiza uralensis*, *Atractylodes* (*A.*) *japonica* and processed *Aconitum carmichaeli*, and this combination of nine herbs has been used in traditional medicine [14,23].

In this study, we aimed to determine whether KCHO-1 can reduce oxidative stress and prevent degeneration of motor neurons in an ALS model. To address this issue, we orally administrated KCHO-1 to $hSOD1^{G93A}$ Tg mice. The KCHO-1 administration delayed disease onset and improved motor activity in symptomatic $hSOD1^{G93A}$ Tg mice. Importantly, we found that KCHO-1 could reduce oxidative stress by reducing $gp91^{phox}$ expression and affecting the MAPK pathway in spinal cords of $hSOD1^{G93A}$ Tg mice, suggesting the therapeutic potential of KCHO-1 for ALS treatment.

Materials and Methods

Animals

The $hSOD1^{G93A}$ Tg mice are hemizygous transgenic B6SJL mice that carry a mutant human SOD1 gene, which has a glycine to alanine base pair mutation at the 93rd codon of the cytosolic Cu/Zn SOD1 [B6SJL−Tg(SOD1 × G93A)1Gur/J]. The transgenic mice used in this study were purchased from the Jackson Laboratory (USA), and that lab specified that the transgenic mice used in this study have an average lifespan of 128.9 ± 9.1 days. For selection of $hSOD1^{G93A}$ Tg mice by genotyping, DNA was extracted from the tail of the mice, and a PCR assay was performed. All mice were housed at a constant temperature of 21°C to 23°C and humidity of 50% to 60% under a 12 h light/dark cycle. Female $hSOD1^{G93A}$ Tg mice were colonized per experimental group (n = 11−12). Mice generally developed disease signs of neuromuscular deficits at an age of 105 to 115 days. All animal experiments were consistent with the guidelines of the Institute of Laboratory Animals Resources (SNU-120821-5-1; Seoul National University, Korea).

Materials

The KCHO-1 used in this study was consistent with that described in a previous study [23]. Briefly, The KCHO-1 was a mixture of herbs, which consists of *C. longa* (HP2013-10-01), *S. miltiorrhiza* (HP2013-10-02), *G. elata* (HP2013-10-03), *Chaenomeles sinensis* (HP2013-10-04), *P. tenuifolia* (HP2013-10-05), *Paeonia japonica* (HP2013-10-06), *Glycyrrhiza uralensis* (HP2013-10-07), *A. japonica* (HP2013-10-08), and processed *Aconitum carmichaeli* (HP2013-10-09). The *C. longa* (4 kg), *S. miltiorrhiza* (4 kg), *G. elata* (4 kg), *Chaenomeles sinensis* (2 kg), *P. tenuifolia* (2 kg), *Paeonia japonica* (2 kg), *Glycyrrhiza uralensis* (2 kg), *A. japonica* (2 kg), and processed *Aconitum carmichaeli* (1 kg) were mixed and extracted in 30% ethanol for 3 h at 84°C to 90°C. The extract was concentrated and lyophilized by using a rotary evaporator. Four marker compounds were selected and selection criteria for the compounds were based on the quantitative method of the Korean Pharmacopeia (Table 1). All specimens were processed and deposited at Hanpoong Pharm & Foods (Korea) [14,23].

Oral delivery of KCHO-1

Toxicity testing of oral-delivered KCHO-1 was previously studied, and there were no reported side effects at the high dose level of 2,000 mg/kg [14]. In this study, KCHO-1 at a dose of 250 mg/kg was treated daily. The age of the transgenic mice at the start of KCHO-1 treatment was 13 weeks and KCHO-1 was administered daily for 4 weeks (mouse ages from 91 days to 119 days).

Behavioral analysis

Before KCHO-1 was delivered to mice, behavioral tests were performed. Prior to testing, the mice underwent a one-week training period to adapt to the apparatus (7650 Accelerating Model, Ugo Basile, Italy). After the training period, 13-week-old

Table 1. Four marker compounds in KCHO-1 were selected with selection criteria based on the quantitative method of the Korean Pharmacopeia

Name	Curcumin	Glycyrrhizic acid	Paeoniflorin	Salvianolic acid B
Chemical formula	$C_{21}H_{20}O_6$	$C_{42}H_{62}O_{16}$	$C_{23}H_{28}O_{11}$	$C_{36}H_{30}O_{16}$
Molar mass	368.38	822.93	480.46	718.62

mice were subjected to a rotarod test. The motor function of a mouse was assessed by measuring the time that a mouse could remain on the apparatus at a rotation rate of 10 rpm. Tests were performed every other day, and the average time for three attempts was recorded for each mouse.

Cell viability assay

The BV2 microglial cells were maintained in Dulbecco's modified Eagle's medium (11995; Gibco, USA) supplemented with 10% FBS (16000; Gibco), 1% penicillin and streptomycin (15140; Gibco). The cells were seeded in 24-well plates. After stabilizing, several concentrations of KCHO-1 were treated (3.1−100 μg/mL). After 24 h, 5 mg/mL MTT solution (Sigma, USA) was treated and the cells were incubated for 4 h at 37°C. The supernatant was discarded and DMSO was added to the BV2 microglial cells to solubilize the formazan crystals. Subsequently, the supernatant was moved to 96-well plates and absorbance was measured by using an EL800 microplate reader (BioTek Instruments, USA) at a wavelength of 540 nm.

Griess assay and ROS test

The BV2 cells were seeded in 24-well plates. After stabilization, the cells were treated with several concentrations (3.1−100 μg/mL) of KCHO-1, and the cells were activated simultaneously with 10 ng/mL lipopolysaccharide (LPS; Sigma) and 10 ng/mL interferon (IFN)-γ (PeproTech, USA). After 24 h, the supernatant was used to determine the nitrite concentration, which was measured by using a colorimetric Griess reagent system according to the manufacturer's instructions (TB229; Promega, USA). Attached cells were used in a ROS test, in which, the cells were treated with CellROX oxidative stress reagents (C10422; Life Technologies, USA) for 30 min at 37°C and then detached by pipetting. Harvested cells were analyzed by performing flow cytometry (BD Bioscience, USA). The ROS test of the spinal cord of $hSOD1^{G93A}$ Tg mice was performed by using H2DCFDA. Cryotissues were sectioned at 10 μm and then stained with H2DCFDA (D399; Thermo Fisher, USA) by treating with 5 μM H2DCFDA for 30 min at 37°C. After 30 min, the ROS level were measured by using an Eclipse TE200 confocal microscope (Nikon, Japan) at 520−610 nm wavelength.

Protein extraction and western blotting analysis

When the mice reached 128 days of age, the spinal cord was extracted and homogenized with a protein extraction kit (PRO-PREP; iNtRON Biotechnology, Korea). After homogenization, the extracted samples were centrifuged at 16,000 × g for 10 min at 4°C. Cells that had been treated with several concentrations of KCHO-1 and activated by 10 ng/mL LPS (Sigma) and 10 ng/mL IFN-γ (PeproTech) were lysed with the protein extraction kit (PRO-PREP; iNtRON Biotechnology). All protein samples were quantified by using a Bio-Rad DC protein assay kit (Bio-Rad Laboratories, USA). For western blotting, equal amounts of each sample were loaded and electrophoresed on 10% to 12% SDS-polyacrylamide gels and then transferred to nitrocellulose membranes. The blots were blocked with 5% bovine serum albumin in TBST for 1 h at room temperature and subsequently incubated with various primary antibodies overnight at 4°C. The following primary antibodies were used: beta-actin (sc-47778; Santa Cruz Biotechnology, USA), GAPDH (No. 2118S; Cell Signaling, USA), anti-GFAP (ab7260; Abcam, UK), anti-iNOS (ab15323; Abcam), anti-$gp91^{phox}$ (ab80508, Abcam), anti p-p38 (No. 9211s; Cell Signaling), and p-ERK1/2 (No. 9121; Cell Signaling). The blots were incubated with peroxidase-conjugated secondary antibodies (1:1000; Invitrogen, USA) and developed with enhanced chemiluminescence reagents (Amersham Pharmacia Biotech, USA). Quantification of all immunoblotting data was performed by using ImageJ v. 1.48 software (National Institutes of Health, USA).

Tissue processing and Immunohistochemistry

At 128 days of mouse age, the mice were transcardially perfused with normal saline followed by 4% paraformaldehyde (PFA) in phosphate-buffered saline (PBS) for fixation. Spinal cord portions (L2-L4) were removed, post-fixed in 4% PFA overnight at 4°C, and transferred to 30% sucrose. The tissues were then embedded into a mold filled with optimum cutting temperature (OCT) compound (Tissue-Tek O.C.T Compound; Sakura Finetek, Japan) and stored at −80°C before cryosectioning. The spinal cords were serially cut on a cryostat into 10 μm thick cross-sections and washed in PBS to remove the OCT compound. After the sections were blocked with 3% to 5% normal goat serum in PBS at room temperature, they were incubated with the primary antibody overnight at 4°C. For detection of the primary antibody, sections were incubated with the appropriate Alexa 488- or 594-conjugated secondary antibodies (1:2,000; Molecular Probes, USA) for 1 h in the dark at room temperature. Images were captured with an Eclipse TE200 confocal microscope (Nikon). To determine the relative immunohistochemical intensity of each signal, ten spinal cord sections per mouse were used (n = 4−5 per group). Each signal was measured in equivalent areas in the anterior horn of the lumbar spinal cord by using ImageJ v. 1.63 software (National Institutes of Health).

Histology

For hematoxylin and eosin (H&E) staining, cryotissues were sectioned at 7 to 8 μm thickness and then stained with H&E by using a standard protocol [9]. The detection of Nissl bodies in the cytoplasm of neurons was performed by Nissl staining. Briefly, the tissues were incubated in 1:1 alcohol/chloroform solution overnight and then immersed in 100% alcohol followed by 95% alcohol and dH_2O for rehydration. The

rehydrated tissues were stained with 0.1% cresyl violet (Sigma-Aldrich, Germany), rinsed, and then slide mounted with coverslips. Fluoro-Jade C (FJC) staining was used to identify degenerating neurons in the CNS. First, the tissues were immersed in 100% alcohol and then 70% alcohol for 3 min each. The tissues were then transferred to 0.06% $KMnO_4$ for 15 min, washed with dH_2O, and stained with a 0.001% FJC solution for 30 min in a dark room. After staining, the slides were rinsed again and mounted with coverslips. Counting Nissl stained or FJC stained motor neurons was performed in equivalent size frames in an anterior horn region, and ten samples were counted per mouse (n = 4–5 per group). All histological examinations were performed by using an Eclipse TE200 confocal microscope (Nikon).

Statistical analysis

Data are presented as mean ± SEM values and were analyzed by using GraphPad 5.0 (GraphPad Software, USA). The immunoblotting data for wild-type, vehicle, and KCHO-1 groups were compared by performing one-way ANOVA. The mean age ± SD of the hSOD1^{G93A} Tg mouse groups were compared by using the Mann-Whitney *U* test for comparisons between two groups. The log-rank test was used for the Kaplan-Meier survival analyses. Comparisons of Griess assay or ROS concentration results were performed by using the Newman-Keuls *post-hoc* test of one-way ANOVA results.

Results

KCHO-1 improves motor activity and delays disease onset in symptomatic hSOD1^{G93A} Tg mice

In these experiments, the rotarod test was performed every second day from post-natal day 91 (panel A in Fig. 1), and three or four mice in each group were randomly sacrificed on day 128, which is the average end-stage day for hSOD1^{G93A} Tg mice. Disease onset was determined when mice first fell from

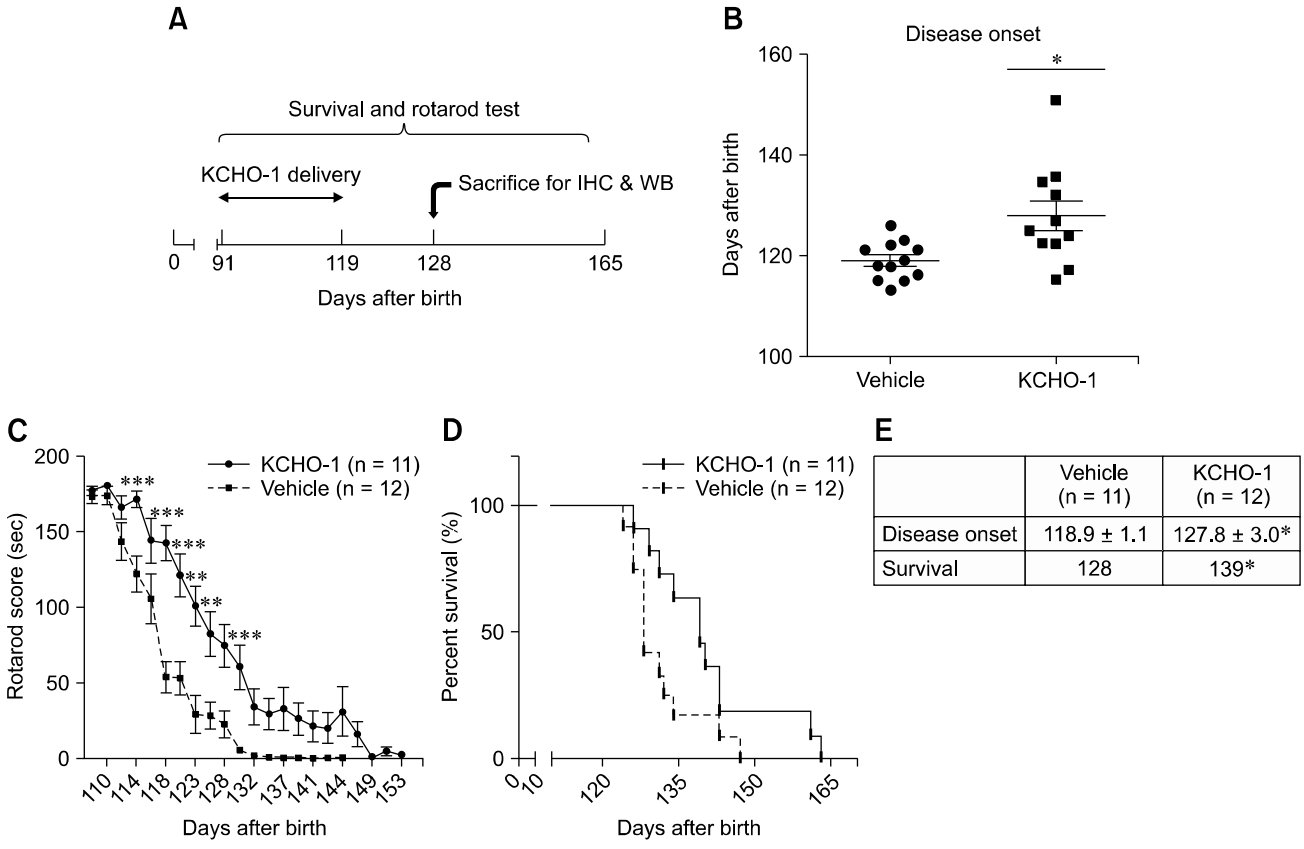

	Vehicle (n = 11)	KCHO-1 (n = 12)
Disease onset	118.9 ± 1.1	127.8 ± 3.0*
Survival	128	139*

Fig. 1. KCHO-1 improved motor function and delayed amyotrophic lateral sclerosis (ALS) disease onset. (A) hSOD1^{G93A} Tg mice (91-days-old) were separated into two groups and treated by oral administration of KCHO-1 (250 mg/kg/day) or normal saline for 4 weeks. At day 128, randomly selected mice (n = 3–4) in each group were sacrificed for other studies. (B) Disease onset was defined as the time when the rotarod test score first began to decrease. KCHO-1 treatment delayed the onset of disease in hSOD1^{G93A} Tg mice. (C) KCHO-1 treatment significantly improved the rotarod score. (D) Mean survival of KCHO-1 treated group was day 139 and that in the vehicle-treated group was day 128. (E) Summary of statistical significance of disease onset and survival rate differences. *$p < 0.05$, **$p < 0.01$, ***$p < 0.001$.

the apparatus during a rotarod test, and the average day of disease onset in the vehicle-treated group was day 118.9 ± 1.1, whereas mean onset in the KCHO-1-treated group was delayed until day 127.8 ± 3.1 (panel B in Fig. 1). These results demonstrate that KCHO-1 treatment could significantly delay disease onset of ALS. As shown in panel C in Fig. 1, the rotarod test results indicate the progression of the disease with KCHO-1-treated mice exhibiting a gradual score decrease, while the rotarod scores of the vehicle-treated group rapidly decreased. In particular, between day 114 and day 130, there were significant differences in the rotarod scores of the two groups. The results demonstrate that KCHO-1-treated mice can withstand decreased motor activity during disease progression. To examine the rates of survival between the two groups, the Kaplan-Meier survival test was performed. In the experiment, the KCHO-1-treated group survived longer than vehicle-treated group. The median survival of the KCHO-1-treated group was 139 days while that for the vehicle-treated group was 128 days (panels D and E in Fig. 1). These results demonstrate that KCHO-1 administration in ALS mice can alleviate disease progression and improve survival rate.

KCHO-1 prevents the degeneration of neurons in the spinal cord of symptomatic hSOD1^{G93A} transgenic mice

To determine whether KCHO-1 administration in ALS mice prevents the degeneration of neuronal cells in the spinal cord, we undertook histological examinations of the anterior horn of the lumbar spinal cord in wild-type, vehicle-, and KCHO-1-treated mice that had been sacrificed on day 128. The spinal cord tissue sections from the three groups were compared by using three different stains. In the first histological examination, H&E staining of spinal cord sections was performed, which indicated that neuronal cell bodies in KCHO-1-treated mice were more numerous than those in the vehicle-treated mice (panel A in Fig. 2). In the second histological examination, we performed Nissl staining of spinal cord sections to identify the Nissl bodies in neurons. The mean numbers of Nissl bodies in the wild-type, vehicle-, and KCHO-1-treated mice were 16.0 ± 1.2, 5.9 ± 0.6, and 11.7 ± 0.6, respectively (panels B and D in Fig. 2). Those staining results indicate that the number of Nissl body-stained neurons in KCHO-1-treated mice was two-fold greater than that in the vehicle-treated mice. Finally, we performed FJC staining, which is used to visualize degenerating neurons via fluorescence microscopy. The FJC stain results for the anterior horn of the spinal cord indicated that the number of degenerating neurons was significantly reduced from 41.5 ± 2.8 per tissue section in the vehicle-treated group to 31.2 ± 1.7 per tissue section after KCHO-1 administration (panels C and E in Fig. 2).

KCHO-1 reduces microglial proliferation and activation

To determine the effect of KCHO-1 administration on microglia and astrocyte distribution in the spinal cord, expression patterns of Iba-1 and glial fibrillary acidic protein (GFAP) were analyzed (panel A in Fig. 3). In the spinal cord, the intensity of Iba-1 expression in microglia was significantly

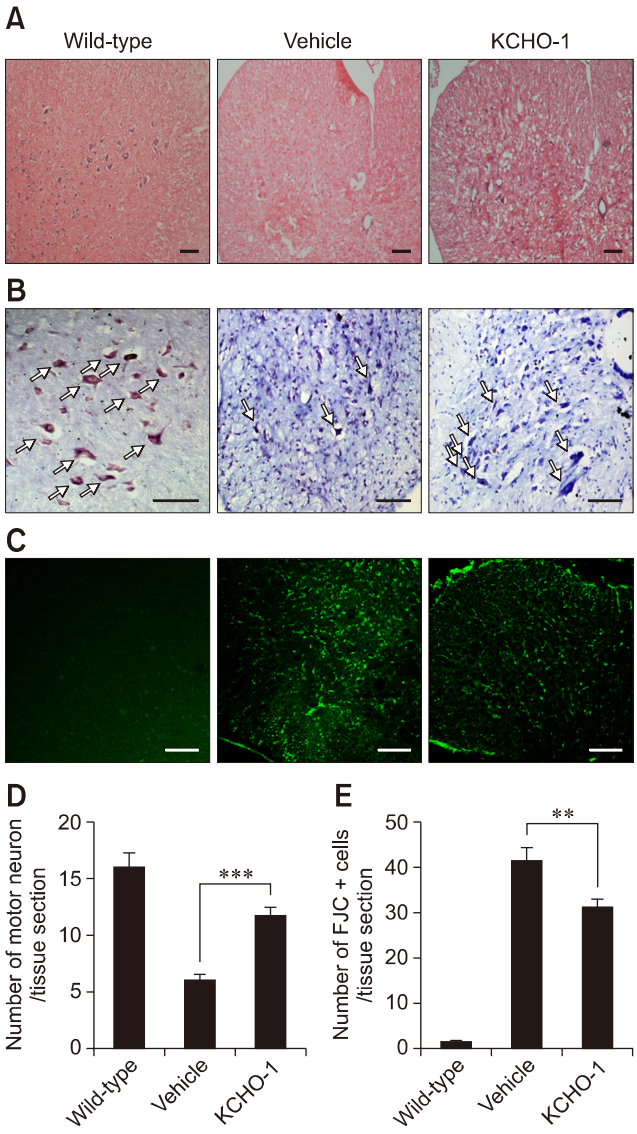

Fig. 2. KCHO-1 treatment improved motor neuron survival in spinal cord of hSOD1^{G93A} Tg mice. (A and B) H&E and Nissl staining show that motor neurons were detected more often in the KCHO-1 treatment group than in the vehicle group. Arrows represent counted number of motor neuron at panel B. (C) Degenerating Fluoro-Jade C-positive neuronal cells (green) are shown in the photograph. Quantification analysis was performed by counting the number of motor neurons or degenerating neurons in the anterior horn of the spinal cords. (D) The number of motor neurons were counted after Nissl staining. (E) The number of degenerating neurons were counted after FJC staining. Data are shown as mean ± SEM values (n = 3–4 per group) and were analyzed by using one-way ANOVA. *p < 0.05, **p < 0.01, ***p < 0.001. H&E stain (A), Nissl stain (B) and Fluoro-Jade C stain (C). Scale bars = 100 μm (A–C).

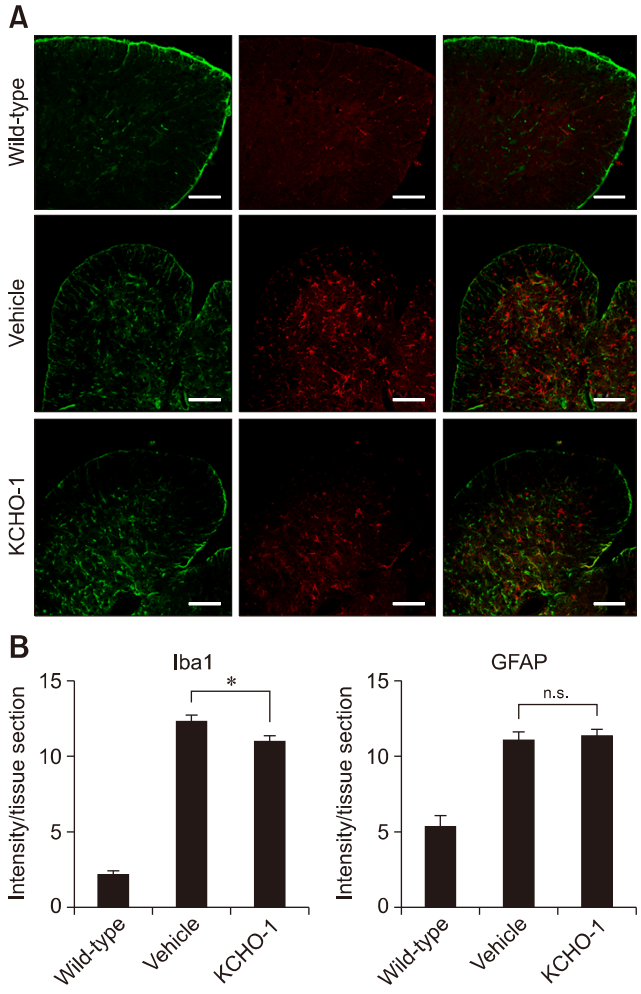

Fig. 3. KCHO-1 reduced microglial proliferation and activation. Expressions levels of Iba1 and GFAP proteins in the anterior horn of spinal cords were compared between wild-type, KCHO-1-treated, and vehicle-treated groups by using immunohistochemistry. (A) Representative images of spinal cord of hSOD1^{G93A} Tg mice showed Iba1-positive microglia (red) and GFAP-positive astrocyte (green) expressions. Compared to the vehicle-treated group, the intensity of Iba1 was significantly reduced in the spinal cord of the KCHO-1-treated group, whereas GFAP intensity was not significantly different. Data are presented as mean ± SEM values and were analyzed by using one-way ANOVA (n = 3–4 per group). *$p < 0.05$. Scale bars = 100 μm (A). n.s., no significant difference.

reduced in the spinal cord of the KCHO-1 group (mean ± SEM; wild-type 2.15 ± 0.3, vehicle 12.32 ± 0.39, and KCHO-1 11.05 ± 0.36), whereas the intensity of GFAP expression, a marker indicative of astrocytes, was not significantly different among the groups (wild-type 5.35 ± 0.6, vehicle 11.05 ± 0.57, and KCHO-1 11.39 ± 0.34) (panel B in Fig. 3). The GFAP expression level was also analyzed by using western blot analysis, the results of which did not show any significant differences among the experimental groups (wild-type 0.5 ± 0.1, vehicle 1.51 ± 0.3, and KCHO-1 1.19 ± 0.2) (Supplementary Fig. 1).

KCHO-1 reduces oxidative stress through gp91^{phox} and MAPK signaling

To investigate the modulation of oxidative stress by KCHO-1 through gp91^{phox} and the MAPK pathway in ALS spinal cord, we first examined the ROS level in the spinal cords of hSOD1^{G93A} Tg mice. As shown in panel A in Fig. 4, the ROS level was reduced in KCHO-1 treated group from that in the vehicle group. Next, we confirmed that the protein levels of inducible nitric oxide synthase (iNOS) and NADPH oxidase (gp91^{phox}) in the spinal cords were readily reduced. The reductions from vehicle-treated to KCHO-1-treated mice were 50% for iNOS (mean ± SEM; wild-type 0.1 ± 0.01, vehicle 0.48 ± 0.04, and KCHO-1 0.25 ± 0.1) and 40% for gp91^{phox} (wild-type 0.23 ± 0.12, vehicle 2.02 ± 0.24, and KCHO-1 1.08 ± 0.13) (panels B and C in Fig. 4). To ascertain that the MAPK pathway was also regulated by KCHO-1, the ERK1/2 and p38 protein levels were examined in the spinal cords. The phosphorylated ERK1 (wild-type 0.28 ± 0.07, vehicle 2.72 ± 0.21, and KCHO-1 1.66 ± 0.31) and ERK2 (wild-type 0.11, vehicle 2.06 ± 0.05, and KCHO-1 1.19 ± 0.14) were significantly reduced by KCHO-1 treatment, but the phosphorylated p38 protein level (wild-type 0.28 ± 0.16, vehicle 1.72 ± 0.11, and KCHO-1 1.19 ± 0.23) was not significantly reduced in the KCHO-1-treated group from that in the vehicle-treated group (panels D and E in Fig. 4).

KCHO-1 reduced oxidative stress in BV2 microglial cells

In order to confirm the effect of KCHO-1 on microglia, we activated BV2 microglial cells by administering 10 ng/mL IFN-γ and 10 ng/mL LPS along with varying concentrations of KCHO-1. The KCHO-1 treatment did not affect cell viability until the 100 μg/mL concentration treatment (panel A in Fig. 5). For analysis of the oxidative level in BV2 microglial cells, we performed Griess and ROS level assays. Activation of microglial cells significantly upregulated the NO_2^- level (mean ± SEM; 17.35 ± 1.27) but KCHO-1 significantly reduced the NO_2^- level at concentrations of 50 μg/mL (12.17 ± 1.65) and 100 μg/mL (10.65 ± 0.97) (panel B in Fig. 5). We also measured the ROS level in activated BV2 microglial cells with or without KCHO-1. The ROS level was significantly increased following treatment of LPS and the IFN-γ in BV2 microglial cells (48.98 ± 3.8) compared to that in the negative control (5.84 ± 0.7), whereas KCHO-1 treatment at 50 and 100 μg/mL concentrations significantly reduced ROS levels (36.74 ± 1.7 and 37.61 ± 1.2, respectively) (panels C and D in Fig. 5).

At several concentrations, KCHO-1 also reduced the iNOS level and the gp91^{phox} protein level in the activated BV2 microglial cells. Notably, the 100 μg/mL of KCHO-1 significantly reduced iNOS (0.65 ± 0.12) and gp91^{phox} (0.6 ±

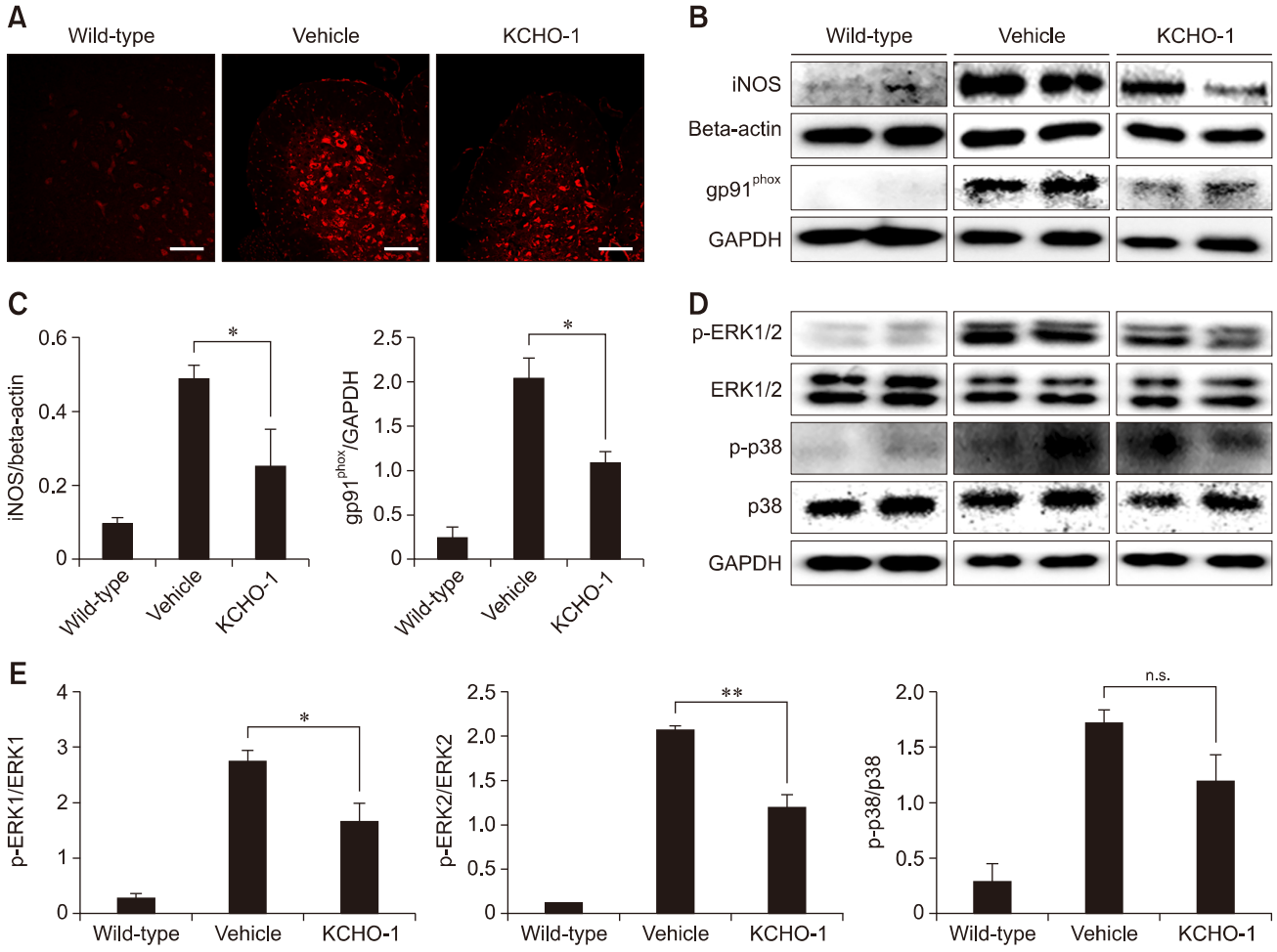

Fig. 4. KCHO-1 reduced oxidative stress through gp91^{phox} and MAPK. (A) Reactive oxygen species (ROS) level in the vehicle group was upregulated in the anterior horn of amyotrophic lateral sclerosis (ALS) spinal cord compared with the wild-type group, and KCHO-1 alleviated the ROS level in the spinal cord compared with that in the vehicle group. (B and C) Western blot images of the expression of inducible nitric oxide synthase (iNOS) and gp91^{phox} were reduced in KCHO-1-treated group compared to that in the vehicle-treated group; wild-type was used as a negative control. (D and E) ERK1/2 and p38 MAPK were measured in the spinal cords of the wild-type, vehicle-, and KCHO-1- treated groups. Phosphorylated ERK1/2 protein level decreased in the KCHO-1-treated group from that in the vehicle-treated group. There was no significant difference in p38 phosphorylation level between the vehicle and KCHO-1 groups. The data are presented as mean ± SEM values and were analyzed by using one-way ANOVA (n = 3–4 per group). *$p < 0.05$, **$p < 0.01$. Scale bars = 100 μm (A). n.s., no significant difference.

0.11) levels from those of activated BV2 microglial cells (iNOS 1.17 ± 0.09, gp91^{phox} 1.32 ± 0.19) (panel E in Fig. 5). To determine the effect of KCHO-1 on the MAPK pathway, we investigated the phosphorylation of p38 and ERK1/2. The LPS and IFN-γ treatment of BV2 cells elevated the phosphorylation of p38 (1.41 ± 0.24) and ERK1/2 (ERK1 1.64 ± 0.24, ERK2 1.33 ± 0.14) from the levels in the negative control (p38 0.07 ± 0.07, ERK2 0.15 ± 0.15). In particular, KCHO-1 at a 100 μg/mL concentration significantly reduced p38 (0.4 ± 0.18) and ERK1 (0.43 ± 0.16) phosphorylation in the activated BV2 microglial cells. KCHO-1 at the same concentration also reduced expression of phosphorylated ERK2 (0.74 ± 0.04), but the reduction was not significant (panel F in Fig. 5).

Discussion

Several previous studies using the herbs included in the compound KCHO-1 have demonstrated that *C. longa*, *C. sinensis*, and *P. tenuifolia* have antioxidant activity [18,19,33], while *S. miltiorrhiza*, *G. elata*, and *A. japonica* have anti-inflammatory or neuroprotective activity [12,15,16,25]. In addition, *P. japonica* and *G. uralensis* prevent fatigue and have antibacterial effects, and *A. carmichaeli* can reduce pain [11,35,37]. These herbs have been used for a long time in

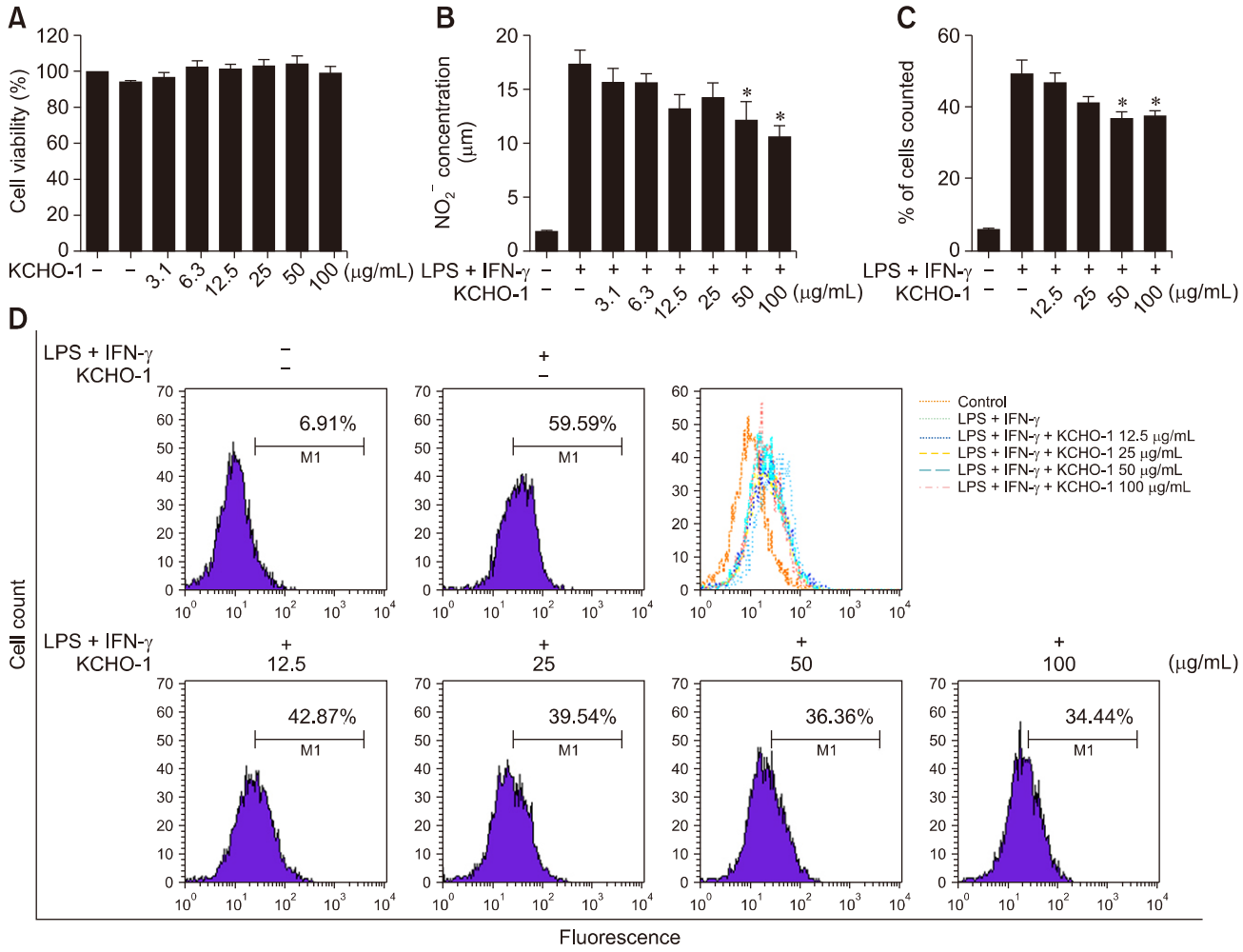

Fig. 5. KCHO-1 reduced oxidative stress in BV2 microglial cells. (A) The KCHO-1 effect at various concentrations on the BV2 cell viability was measured by MTT assay. (B) The concentration of nitric oxide released by activated microglial cells were reduced by KCHO-1 treatment, and the KCHO-1 concentrations of 50 and 100 μg/mL reduced nitric oxide level significantly. (C and D) Microglial cell were classically activated with or without various concentrations of KCHO-1, and ROS were measured by flow cytometry. KCHO-1 at 50 and 100 μg/mL concentrations significantly reduced ROS level in activated microglial cells. (E) The KCHO-1 treatment down-regulated an inducible nitric oxide synthase (iNOS) and $gp91^{phox}$ protein levels; notably, the 100 μg/mL KCHO-1 concentration significantly reduced iNOS and $gp91^{phox}$ protein levels in the activated microglial cells. (F) Classically activated microglial cells were treated with various concentrations of KCHO-1 and MAPK protein expression was determined by western blotting. Extracellular signal-regulated kinase (ERK)1 phosphorylation were significantly reduced with 100 μg/mL KCHO-1 treatment, but ERK2 phosphorylation was not significantly reduced. The phosphorylated form of p38 was also significantly reduced at 100 μg/mL of KCHO-1. Densitometry values of western blots were normalized to glyceraldehyde 3-phosphate dehydrogenase (GAPDH) or total form value. Data are presented as mean ± SEM values from three independent experiments. *$p < 0.05$ compared with the LPS + IFN-γ (+) or KCHO-1 (−) group. LPS, lipopolysaccharide, IFN-γ, interferon-gamma.

traditional medicine and have been studied for the treatment of many diseases [10-12,15,16,18,19,25,33,35,37]. In this study, we found that motor function and survival rate improved and disease onset delayed in KCHO-1-treated $hSOD1^{G93A}$ Tg mice. Furthermore, KCHO-1 administration reduced neuronal loss in the spinal cord of $hSOD1^{G93A}$ Tg mice. Because oxidative stress is a main pathological hallmark of ALS, we focused on the effect of KCHO-1 on reducing oxidative stress [1]. To determine the antioxidant effect of KCHO-1, we studied glial cells, particularly microglia and astrocytes, which play an important role in neurodegeneration. The expression level of Iba-1 was reduced in the spinal cords of the KCHO-1-treated group, whereas expression of the astrocyte marker GFAP was not reduced. These results indicated that KCHO-1 can reduce proliferation of microglia but not astrocytes. Astrocytes are a major source of anti- and pro-inflammatory cytokines, and they

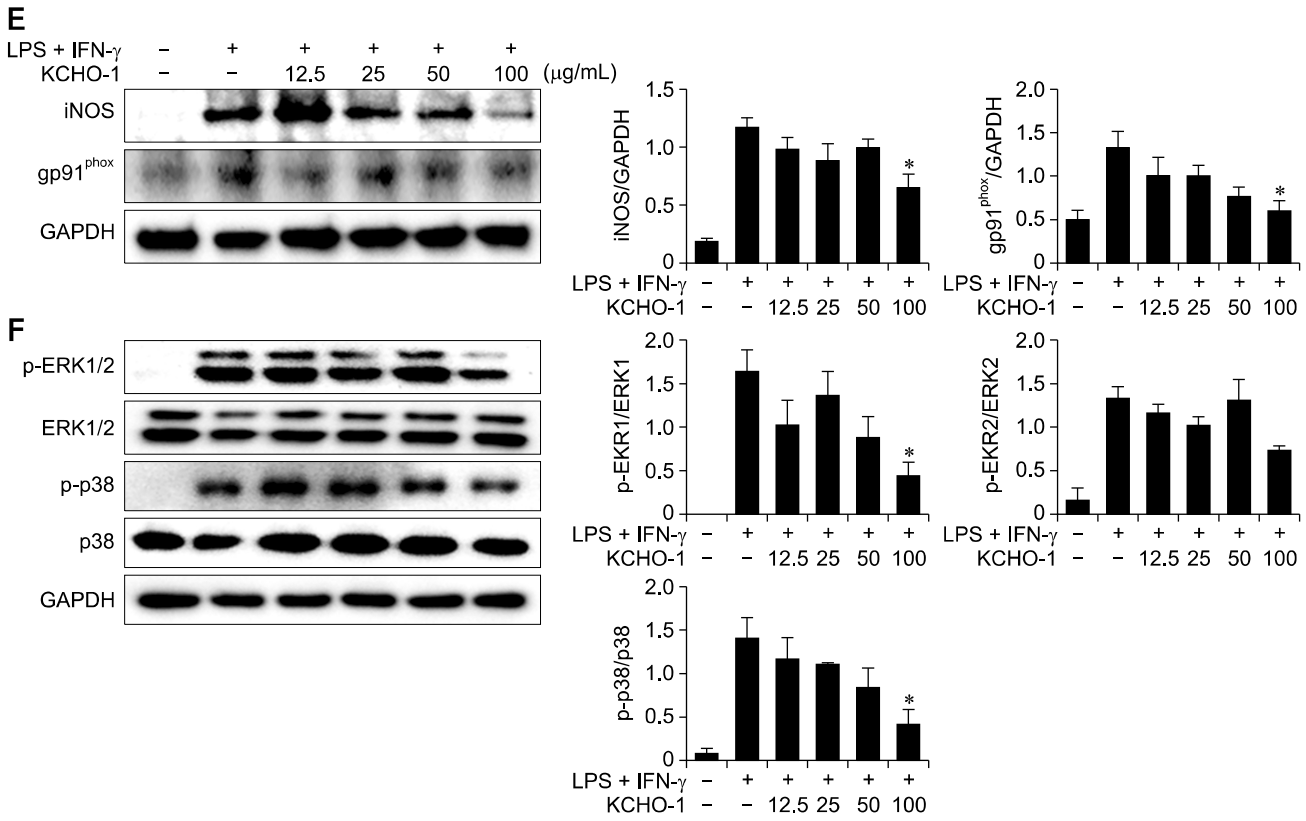

Fig. 5. Continued.

contribute to the immune response in the CNS. Previously, astrogliosis, activation, and especially upregulation of GFAP have been observed in the spinal cords of ALS patients. However, the mechanism of astrogliosis in ALS remains unclear. Our data showed that KCHO-1 administration improved motor function, survival rate, and disease onset in hSOD1^{G93A} Tg mice without down-regulating GFAP. Microglia, another type of glial cell, are the immune cells of the CNS, and abnormal activation of these cells influences oxidative stress that regulates the pathological environment in ALS [20,39]. In previous studies, the gp91^{phox} subunit of NADPH oxidase was stimulated by mutant SOD1 protein in the microglia of hSOD1^{G93A} Tg mice, and these cells over-produce ROS through NADPH oxidase [2,4,36]. Overexpressed gp91^{phox} protein is a main cause of ROS, but that alone does not have a significant effect on neuronal death. When NADPH oxidase is expressed with iNOS in microglia, the simultaneous activation releases many neurotoxic factors and contributes significantly to oxidative stress [7,27,34]. On that basis, we examined whether the expression of gp91^{phox} and iNOS protein were decreased in the spinal cords of hSOD1^{G93A} Tg mice following KCHO-1 treatment, and our data showed that KCHO-1 reduced oxidative stress in the spinal cord through gp91^{phox} and iNOS down-regulation.

Furthermore, gp91^{phox}-increased oxidative stress in the spinal cord may activate the MAPK pathway, which is known to be a cell stress signaling pathway in the CNS of ALS [1]. In this study, we investigated p38 and ERK1/2 activity and observed that KCHO-1 at several concentrations could alleviate activation of p38 and ERK1/2 in classically activated microglial cells, along with gp91^{phox} and iNOS down-regulation. Consistently, in the hSOD1^{G93A} Tg mice, the phosphorylated form of ERK1/2 was decreased in the KCHO-1 treated group, but the phosphorylated p38 level was not significantly reduced in the KCHO-1 treated group compared to that in the vehicle group. The p38 protein, as a downstream effector of a stress signaling pathway, is activated by various factors in ALS. Particularly, the p38-MAPK pathway can be activated by mutant SOD1 proteins, other inflammatory factors, and by oxidative stress in the astrocytes of ALS. The insignificant downregulation of p38 in the KCHO-1 treatment group may be associated with the lack of a significant effect on astrocytes in the spinal cords of the KCHO-1 group [3,17]. Therefore, further study is required to elucidate the relationship between the p38-MAPK pathway and the KCHO-1 effect in ALS.

In previous study, it was demonstrated that KCHO-1 can alleviate inflammation via the nuclear factor kappa B pathway in BV2 microglial cells [23] and reduce oxidative stress via

HO-1 upregulation [23]. In the present study, we observed that KCHO-1 can alleviate oxidative stress through gp91^{phox} and the MAPK pathway in classically activated microglial cells. Moreover, we have shown that these effects can be elicited in hSOD1^{G93A} Tg mice, thereby improving the progression of ALS. Therefore, KCHO-1 can be considered as a new agent for treatment of ALS.

Acknowledgments

This study was supported by the Traditional Korean Medicine R&D Program funded by the Ministry of Health & Welfare through the Korea Health Industry Development Institute (KHIDI) (HI11C2142) and partially supported by the Research Institute for Veterinary Science, Seoul National University, Republic of Korea.

Conflict of Interest

The authors declare no conflicts of interest.

References

1. **Apolloni S, Parisi C, Pesaresi MG, Rossi S, Carrì MT, Cozzolino M, Volonté C, D'Ambrosi N.** The NADPH oxidase pathway is dysregulated by the P2X7 receptor in the SOD1-G93A microglia model of amyotrophic lateral sclerosis. J Immunol 2013, **190**, 5187-5195.
2. **Barber SC, Shaw PJ.** Oxidative stress in ALS: key role in motor neuron injury and therapeutic target. Free Radic Biol Med 2010, **48**, 629-641.
3. **Ben Haim L, Carrillo-de Sauvage MA, Ceyzériat K, Escartin C.** Elusive roles for reactive astrocytes in neurodegenerative diseases. Front Cell Neurosci 2015, **9**, 278.
4. **Boillée S, Cleveland DW.** Revisiting oxidative damage in ALS: microglia, Nox, and mutant SOD1. J Clin Invest 2008, **118**, 474-478.
5. **Bordt EA, Polster BM.** NADPH oxidase- and mitochondria-derived reactive oxygen species in proinflammatory microglial activation: a bipartisan affair? Free Radic Biol Med 2014, **76**, 34-46.
6. **Bozzo F, Mirra A, Carrì MT.** Oxidative stress and mitochondrial damage in the pathogenesis of ALS: new perspectives. Neurosci Lett 2017, **636**, 3-8.
7. **Brown GC, Neher JJ.** Inflammatory neurodegeneration and mechanisms of microglial killing of neurons. Mol Neurobiol 2010, **41**, 242-247.
8. **Bucchia M, Ramirez A, Parente V, Simone C, Nizzardo M, Magri F, Dametti S, Corti S.** Therapeutic development in amyotrophic lateral sclerosis. Clin Ther 2015, **37**, 668-680.
9. **Cardiff RD, Miller CH, Munn RJ.** Manual hematoxylin and eosin staining of mouse tissue sections. Cold Spring Harb Protoc 2014, **2014**, 655-658.
10. **Du H, Wu J, Li H, Zhong PX, Xu YJ, Li CH, Ji KX, Wang LS.** Polyphenols and triterpenes from *Chaenomeles* fruits: chemical analysis and antioxidant activities assessment. Food Chem 2013, **141**, 4260-4268.
11. **Hong JA, Chung SH, Lee JS, Kim SS, Shin HD, Kim H, Jang MH, Lee TH, Lim BV, Kim YP, Kim CJ.** Effects of *Paeonia radix* on 5-hydroxytryptamine synthesis and tryptophan hydroxylase expression in the dorsal raphe of exercised rats. Biol Pharm Bull 2003, **26**, 166-169.
12. **Hong MH, Kim JH, Bae H, Lee NY, Shin YC, Kim SH, Ko SG.** *Atractylodes japonica* Koidzumi inhibits the production of proinflammatory cytokines through inhibition of the NF-κB/IκB signal pathway in HMC-1 human mast cells. Arch Pharm Res 2010, **33**, 843-851.
13. **Hooten KG, Beers DR, Zhao W, Appel SH.** Protective and toxic neuroinflammation in amyotrophic lateral sclerosis. Neurotherapeutics 2015, **12**, 364-375.
14. **Jeong H, Lee J, Cha E, Park M, Son I, Song B, Kim S.** A study on the oral toxicity of mecasin in rats. J Pharmacopuncture 2014, **17**, 61-65.
15. **Jiang WY, Jeon BH, Kim YC, Lee SH, Sohn DH, Seo GS.** PF2401-SF, standardized fraction of *Salvia miltiorrhiza* shows anti-inflammatory activity in macrophages and acute arthritis *in vivo*. Int Immunopharmacol 2013, **16**, 160-164.
16. **Kim BW, Koppula S, Kim JW, Lim HW, Hwang JW, Kim IS, Park PJ, Choi DK.** Modulation of LPS-stimulated neuroinflammation in BV-2 microglia by *Gastrodia elata*: 4-hydroxybenzyl alcohol is the bioactive candidate. J Ethnopharmacol 2012, **139**, 549-557.
17. **Kim EK, Choi EJ.** Pathological roles of MAPK signaling pathways in human diseases. Biochim Biophys Acta 2010, **1802**, 396-405.
18. **Kim KS, Lee DS, Bae GS, Park SJ, Kang DG, Lee HS, Oh H, Kim YC.** The inhibition of JNK MAPK and NF-kappaB signaling by tenuifoliside A isolated from *Polygala tenuifolia* in lipopolysaccharide-induced macrophages is associated with its anti-inflammatory effect. Eur J Pharmacol 2013, **721**, 267-276.
19. **Kim Y, You Y, Yoon HG, Lee YH, Kim K, Lee J, Kim MS, Kim JC, Jun W.** Hepatoprotective effects of fermented *Curcuma longa* L. on carbon tetrachloride-induced oxidative stress in rats. Food Chem 2014, **151**, 148-153.
20. **Kobayashi K, Imagama S, Ohgomori T, Hirano K, Uchimura K, Sakamoto K, Hirakawa A, Takeuchi H, Suzumura A, Ishiguro N, Kadomatsu K.** Minocycline selectively inhibits M1 polarization of microglia. Cell Death Dis 2013, **4**, e525.
21. **Kwiatkowski TJ Jr, Bosco DA, LeClerc AL, Tamrazian E, Vanderburg CR, Russ C, Davis A, Gilchrist J, Kasarskis EJ, Munsat T, Valdmanis P, Rouleau GA, Hosler BA, Cortelli P, de Jong PJ, Yoshinaga Y, Haines JL, Pericak-Vance MA, Yan J, Ticozzi N, Siddique T, McKenna-Yasek D, Sapp PC, Horvitz HR, Landers JE, Brown RH Jr.** Mutations in the *FUS*/*TLS* gene on chromosome 16 cause familial amyotrophic lateral sclerosis. Science 2009, **323**, 1205-1208.
22. **Lee DS, Ko W, Song BK, Son I, Kim DW, Kang DG, Lee HS, Oh H, Jang JH, Kim YC, Kim S.** The herbal extract KCHO-1 exerts a neuroprotective effect by ameliorating oxidative stress via heme oxygenase-1 upregulation. Mol Med Rep 2016, **13**, 4911-4919.
23. **Lee DS, Ko W, Yoon CS, Kim DC, Yun J, Lee JK, Jun KY, Son I, Kim DW, Song BK, Choi S, Jang JH, Oh H, Kim S, Kim YC.** KCHO-1, a novel antineuroinflammatory agent,

inhibits lipopolysaccharide-induced neuroinflammatory responses through Nrf2-mediated heme oxygenase-1 expression in mouse BV2 microglia cells. Evid Based Complement Alternat Med 2014, **2014**, 357154.
24. **Liao B, Zhao W, Beers DR, Henkel JS, Appel SH.** Transformation from a neuroprotective to a neurotoxic microglial phenotype in a mouse model of ALS. Exp Neurol 2012, **237**, 147-152.
25. **Manavalan A, Ramachandran U, Sundaramurthi H, Mishra M, Sze SK, Hu JM, Feng ZW, Heese K.** *Gastrodia elata* Blume (tianma) mobilizes neuro-protective capacities. Int J Biochem Mol Biol 2012, **3**, 219-241.
26. **Marden JJ, Harraz MM, Williams AJ, Nelson K, Luo M, Paulson H, Engelhardt JF.** Redox modifier genes in amyotrophic lateral sclerosis in mice. J Clin Invest 2007, **117**, 2913-2919.
27. **Mungrue IN, Husain M, Stewart DJ.** The role of NOS in heart failure: lessons from murine genetic models. Heart Fail Rev 2002, **7**, 407-422.
28. **Murdock BJ, Bender DE, Segal BM, Feldman EL.** The dual roles of immunity in ALS: injury overrides protection. Neurobiol Dis 2015, **77**, 1-12.
29. **Neumann M, Sampathu DM, Kwong LK, Truax AC, Micsenyi MC, Chou TT, Bruce J, Schuck T, Grossman M, Clark CM, McCluskey LF, Miller BL, Masliah E, Mackenzie IR, Feldman H, Feiden W, Kretzschmar HA, Trojanowski JQ, Lee VMY.** Ubiquitinated TDP-43 in frontotemporal lobar degeneration and amyotrophic lateral sclerosis. Science 2006, **314**, 130-133.
30. **Palomo GM, Manfredi G.** Exploring new pathways of neurodegeneration in ALS: the role of mitochondria quality control. Brain Res 2015, **1607**, 36-46.
31. **Pasinelli P, Brown RH.** Molecular biology of amyotrophic lateral sclerosis: insights from genetics. Nat Rev Neurosci 2006, **7**, 710-723.
32. **Rosen DR, Siddique T, Patterson D, Figlewicz DA, Sapp P, Hentati A, Donaldson D, Goto J, O'Regan JP, Deng HX, Rahmani Z, Krizus A, McKennna-Yasek D, Cayabyab A, Gaston SM, Berger R, Tanzi RE, Halperin JJ, Herzfeldt B, Van den Bergh R, Hung WY, Bird T, Deng G, Mulder DW, Smyth C, Laing NG, Soriano E, Pericak-Vance MA, Haines J, Rouleau GA, Gusella JS, Horvitz HR, Brown RH Jr.** Mutations in Cu/Zn superoxide dismutase gene are associated with familial amyotrophic lateral sclerosis. Nature 1993, **362**, 59-62.
33. **Sancheti S, Sancheti S, Seo SY.** Antidiabetic and antiacetylcholinesterase effects of ethyl acetate fraction of *Chaenomeles sinensis* (Thouin) Koehne fruits in streptozotocin-induced diabetic rats. Exp Toxicol Pathol 2013, **65**, 55-60.
34. **Takeuchi A, Isobe KI, Miyaishi O, Sawada M, Fan ZH, Nakashima I, Kiuchi K.** Microglial NO induces delayed neuronal death following acute injury in the striatum. Eur J Neurosci 1998, **10**, 1613-1620.
35. **Villinski JR, Bergeron C, Cannistra JC, Gloer JB, Coleman CM, Ferreira D, Azelmat J, Grenier D, Gafner S.** Pyrano-isoflavans from *Glycyrrhiza uralensis* with antibacterial activity against *Streptococcus mutans* and *Porphyromonas gingivalis*. J Nat Prod 2014, **77**, 521-526.
36. **Wu DC, Ré DB, Nagai M, Ischiropoulos H, Przedborski S.** The inflammatory NADPH oxidase enzyme modulates motor neuron degeneration in amyotrophic lateral sclerosis mice. Proc Natl Acad Sci U S A 2006, **103**, 12132-12137.
37. **Xu H, Arita H, Hayashida M, Zhang L, Sekiyama H, Hanaoka K.** Pain-relieving effects of processed *Aconiti* tuber in CCI-neuropathic rats. J Ethnopharmacol 2006, **103**, 392-397.
38. **Yang EJ, Jiang JH, Lee SM, Yang SC, Hwang HS, Lee MS, Choi SM.** Bee venom attenuates neuroinflammatory events and extends survival in amyotrophic lateral sclerosis models. J Neuroinflammation 2010, **7**, 69.
39. **Zhang F, Jiang L.** Neuroinflammation in Alzheimer's disease. Neuropsychiatr Dis Treat 2015, **11**, 243-256.
40. **Zhao W, Beers DR, Appel SH.** Immune-mediated mechanisms in the pathoprogression of amyotrophic lateral sclerosis. J Neuroimmune Pharmacol 2013, **8**, 888-899.